12

Underwater Acoustic Detection and Signal Processing Near the Seabed

Henry M. Manik
Department of Marine Science and Technology Faculty of Fisheries and Marine Sciences, Bogor Agricultural University Kampus IPB Darmaga Bogor 16680 Indonesia

1. Introduction

1.1 Background

Underwater acoustic instruments has been an indispensable tool to study the ocean. Echo sounder is one of the acoustic instrument used to remotely classify distributions of biological organisms such as fish and plankton (MacLennan and Simmonds, 1992; Furusawa, 2000). Knowledge of species, location, and behavior observed by the sounders are important for fisheries, fisheries management, and ecological studies.

Echo sounders have also been used to characterize the sea bottom type such as rocks, sand, and mud (Stanton, 1994). The characterization of the sea bottom type are useful in applications such as fish habitat study, fishing port construction, geological studies, marine exploration, and mining.

With the end of World War II, studies on underwater acoustics for sea bottom interactions began extensively. Urick (1954) defined the measure of *backscatter strength* as the ratio of scattered energy to incident energy per unit area, per unit solid angle and this quantity was expressed in decibels. Urick used the frequencies of 10 to 60 kHz to measure the backscattering from the harbor bottom. Mackenzie (1961) published the results for lower frequency scattering in deep water and introduced empirical Lambertian backscatter coefficient which was to be cited often in subsequent studies. McKinney and Anderson (1964) investigated potential scattering mechanism based on the interface relief and sediment particle.

One of the methods to measure the bottom backscattering strength is to use the echo integration method (Aoyama *et al*, 1999). This method is used as the main tool for quantifying the abundance of marine fish or planktonic organisms. The echo integration output can be converted to biomass. For the general situation of arbitrary density, as with a school of fish, individual target echoes may not be resolvable. In this case, the echo voltage, after detection and application of suitable range compensation, is squared and summed over a defined interval. The resulting quantity is proportional to the volume or area backscattering coefficient. Division of this by the characteristic backscattering cross section for the target fish yields the numerical density. The echo integration technique has been originally used for fisheries surveys and at the present study we adopted it to measure backscattering strength (SS) of the sea bottom.

Acoustic scattering by the sea bottom has been studied in order to either predict the performance of the echosounder system (Aoyama, *et al*. 1999) or to quantitatively map the

sea bottom. Characterization of sea bottom can be obtained by measuring the bottom backscattering strength (SS). From the measured SS we may be able to estimate the fish habitat.

1.2 Research objectives

The objectives of this researches are development and application of methods to characterize or quantify the fish and sea bottom by underwater acoustic instrument originally developed for measurements of fish scattering. More specifically, the objective is to extensively use multi frequency acoustics (38, 70, and 120 kHz) to measure the bottom backscattering strength (SS) and fish quantification in off Southern Jawa Island, Indonesia.
The SS can be measured by the bottom scattering theory developed by Aoyama *et al*. (1999). As the extension of this theory, a simple but powerful model for bottom scattering, that is a ring surface scattering (RSS) model was developed. The RSS model enables to interpret the bottom echo and to measure the SS value. The SS values, measured for the first time at the sea off Jawa Island, are related to the sounder frequency, beam width, and the bottom type and the properties of the SS with respect to the parameters are examined. The bottom material sampling were conducted to interpret the bottom echo. An associated objective of this study is to measure bottom depth to know the bottom topography.
The other objective is to identify the bottom material by the SS value and relate it to bottom fish habitat. We developed a new and effective method to display fish volume scattering and bottom SS simultaneously. To verify the bottom fish echo, the bottom trawling was conducted.

2. Bottom scattering models

2.1 Preface

A number of mathematical models have been developed in order to gain a better physical understanding of acoustic backscattering from the sea bottom. By observing echo fluctuations from sea bottom, Stanton (1985) determined quantitative information of bottom relief such as bottom roughness. He extended the Eckart (1953) acoustic scattering theory to show the relationship between the probability density function of the echo level and the rms roughness. Stanton model is plane wave model. Jackson *et al*. (1986) developed a bottom scattering model using the composite roughness and grazing angle parameters.
Aoyama et al. (1997) model was extended as ring surface scattering model (RSS model) in this Chapter. The extension of this model from Aoyama et al. model is described. The RSS model exhibits a raw backscattering strength (without averaging) at the peak of bottom echoes and easily convert the bottom scattering strength to the bottom backscattering strength (SS). Aoyama et al. used the approximation method for the equivalent beam angle, but the RSS model uses a strict instantaneous equivalent beam angle for surface scattering.

2.2 Normal incident bottom scattering theory

Normal incidence reflection of sound from the sea bottom is relatively easy to detect. It is used in depth sounders to give the water depth for ships and boats. There has been, however, little research a bottom backscattering strength measurement by normal incidence echo sounders.

Because the wave is propagating, a certain amount of power flow across a unit area normal to the direction of the propagation. This amount of power is called the sound intensity and shown as

$$I = \frac{P^2}{\rho\, c} \tag{2.1}$$

where P is the pressure, ρ is the water density, and c is the sound speed in water.
Sound intensity of surface scattering from a small scattering area, dS is shown by

$$dI = I_o\, r^{-4} \exp(-4\alpha\, r)\, b^2\, S_S\, dS \tag{2.2}$$

where I_o is the source acoustic intensity, r is the range from transducer to the elemental scattering area, dS, α is the absorption coefficient, b is the directivity function of the transducer, and Ss is the bottom backscattering strength (Fig. 2.1). In decibel notation SS = 10 log Ss.
From Fig. 2.1, we have

$$dS = \frac{r\, d\theta}{\cos\theta}\; r \sin\theta = r^2 \tan\theta\, d\theta\, d\phi \tag{2.3}$$

where θ and ϕ are the polar and azimuthal angles, respectively.
Substitution of Eq. (2.3) into Eq. (2.2) yields

$$dI = I_o\, r^{-2} \exp(-4\alpha\, r)\, b^2\, S_S \tan\theta\, d\theta\, d\phi \tag{2.4}$$

Intensity of the surface backscattering strength, I, is the total of dI, therefore

$$I = \int dI \tag{2.5}$$

In general, the S_S becomes smaller when the incident angle, θ become higher. For the quantitative echo sounder with the narrow beam, however, the effect of θ to the scattering should be negligible. Therefore, Eq. (2.5) can be written as

$$I = I_o\, r^{-2} \exp(-4\,\alpha\, r)\, S_S\, \Phi \tag{2.6}$$

where

$$\Phi = \int_0^{2\pi} \int_{\theta_1}^{\theta_2} b^2 \tan\theta\, d\theta\; d\phi \tag{2.7}$$

and Φ is called the equivalent beam angle for surface scattering.
The integration limits θ_1 and θ_2 depend on the time or slant range, r, from the transducer to elemental scattering area and shown as

$$\theta_1 = \begin{cases} 0 & (R \le r < R + c\,\tau/2) \\ \cos^{-1}\left(\dfrac{R}{r - c\,\tau/2}\right) & (r \ge R + c\,\tau/2) \end{cases}$$

and

$$\theta_2 = \cos^{-1}\left(\frac{R}{r}\right) \tag{2.8}$$

where R is the range from the transducer to the sea bottom, c is the sound speed, and τ is the pulse width. For a circular piston transducer, the directivity of transducer is given by

$$b(\theta) = \left(\frac{2\,J_1\,(ka\sin\theta)}{ka\sin\theta}\right)^2 \tag{2.9}$$

where J_1 is the first order of the first kind Bessel function, $k = 2\pi/\lambda$, k is the wave number and λ is the wave length, and a is the radius of the transducer.

2.3 Ring surface scattering model

We derived a new model called " ring surface scattering model " from the above theory. This model enables us to measure the bottom backscattering strength (SS) by using the echo sounder (Aoyama, *et al*., 1999). Figure 2.3 shows a simplified block diagram for bottom backscattering measurement by underwater acoustic instrument.

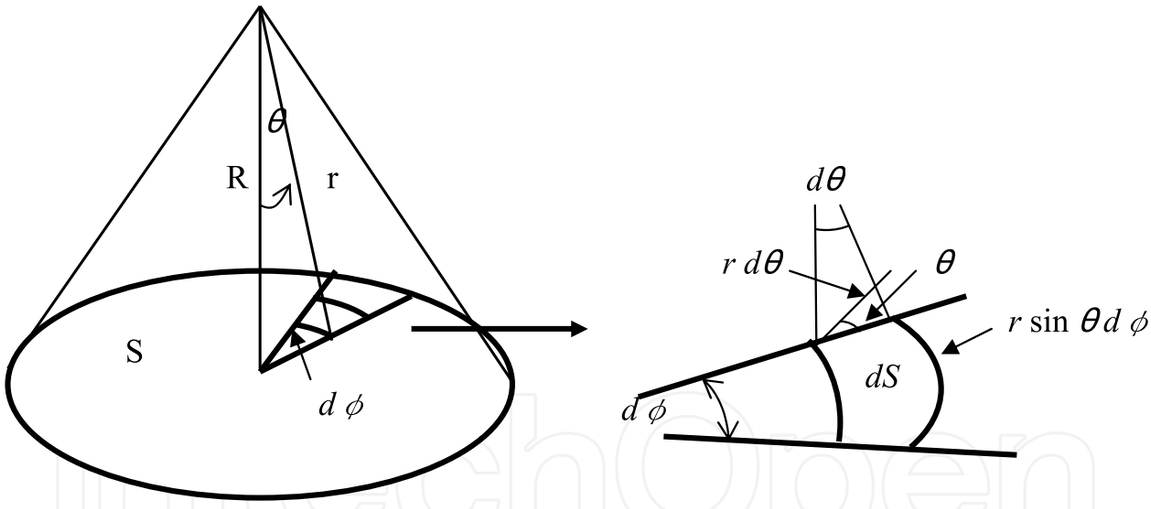

Fig. 2.1. Principle of surface scattering.

Figure 2.2 shows the geometry showing change of scattering plane with time.The surface insonified by the pulse changes from a circle (a) toa circular (b) like ring with time.
The backscattered pressure signal from the bottom received by the transducer (Fig. 2.3), $P_{RB,}$

$$P_{RB}^2 = P_o\, r^{-2}\, exp(-4a\, r)\, \Phi\, S_S \tag{2.10}$$

where P_o is the source pressure level.
The bottom echo signal is amplified by the amplifier to give

$$E_{RB} = P_{RB}\, M\, G_R \tag{2.11}$$

where E_{RB} is the echo amplitude at the preamplifier output, M is the receiving sensitivity of the transducer, and G_R is the preamplifier gain.
The echo amplitude, E_{RB}, is shown from Eqs. (2.10) and (2.11) as

$$E_{RB}^2 = K_{TR}^2 \, r^{-2} \exp(-4\alpha \, r) \, \Phi \, S_S \tag{2.12}$$

where $K_{TR} = P_o \, M \, G_R$ is the transmitting receiving coefficient. In this reduction we assumed $r \simeq R$ except for r and R in Φ (Eq. 2.7).
The time varied gain (TVG) amplifier output of E_{RB} corrected for an absorption and spreading losses, E_{TB}, is

$$E_{TB} = G_{TM} \, r \exp(2\alpha \, r) E_{RB} \tag{2.13}$$

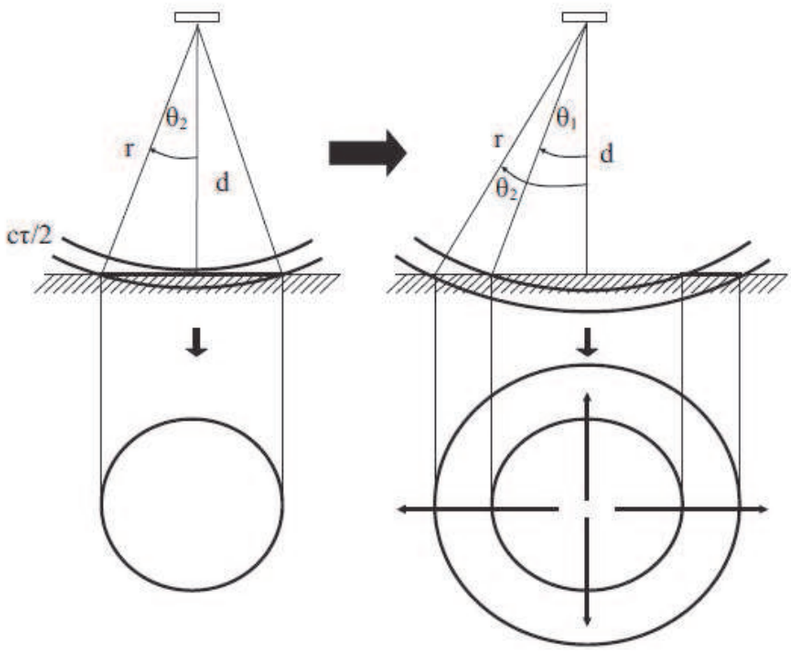

(a) circle surface **(b) circular rings**

Fig. 2.2. Geometry showing change of scattering plane with time. The acoustic wave hit the bottom at the bold lines.

where G_{TM} is the coefficient for the 20 log r TVG amplifier gain. From Eqs. (2.12) and (2.13) we obtain

$$E_{TB}{}^2 = (K_{TR} G_{TM})^2 \Phi \, Ss \, . \tag{2.14}$$

The "raw" SV value of the bottom echo, S_{VB} , is

$$S_{VB} = \frac{E_{TB}{}^2}{K_M{}^2} \tag{2.15}$$

where K_M is the multiple echo coefficient and given by

$$K_M{}^2 = \left(K_{TR} G_{TM}\right)^2 \Psi\left(c\tau / 2\right) \tag{2.16}$$

where

$$\Psi = \int_0^{2\pi} \int_0^{\pi/2} b^2 \sin\theta \, d\theta \, d\phi \tag{2.17}$$

The above Ψ is the equivalent beam angle of the volume scattering.
Substitution of E_{TB} of Eq. (2.14) and K_M of Eq. (2.16) into Eq. (2.15) yields

$$S_{VB} = \frac{Ss\, \Phi}{\Psi\left(c\,\tau / 2\right)} \tag{2.18}$$

This equation is called " *ring surface scattering model* ".
The echo wave form simulation is possible by this model. The results of the wave form simulation are compared with the wave forms from the actual data obtained by the echo sounder to interpret the data. When our purpose is to simulate the wave form and echo level, we use the instantaneous equivalent beam angle Φ, Eq. (2.7), as a function of range.

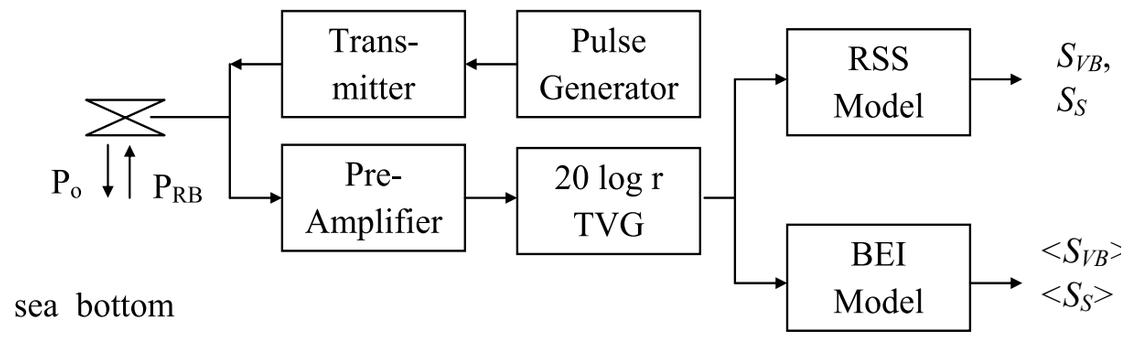

Fig. 2.3. The simplified block diagram of underwater acoustic instrument to measure bottom backscattering strength (SS). RSS is ring surface scattering and BEI is bottom echo integration.

2.4 Bottom echo integration

In the bottom echo integration method (Aoyama, *et al.*, 1999) we average the bottom echoes for a predefined depth layer (r to $r + r_w$) including the bottom echoes and for a ping sequence to obtain the average bottom echo integration strength.
The average squared voltage of TVG outputs with respect to the ping (index i) and the range is

$$\left\langle E_{TB}{}^2 \right\rangle = \frac{1}{r_w} \int_r^{r+r_w} \left(\frac{1}{m} \sum_{i=1}^{m} E_{TBi}{}^2 \right) dr \tag{2.19}$$

where m is the integration period in ping. The average bottom echo integration strength ("bottom SV"), $< S_{VB} >$, is obtained as done in the ordinary echo integration method :

$$\langle S_{VB} \rangle = \frac{\langle {E_{TB}}^2 \rangle}{{K_M}^2} \tag{2.20}$$

Substitution of the Eq. (2.19) into Eq. (2.20) yield

$$\langle S_{VB} \rangle = \left(\frac{K_{TR} G_{TM}}{K_M} \right)^2 \frac{1}{r_w} \int_r^{r+r_w} \left[\frac{1}{m} \sum_{i=1}^{m} \Phi_i \, Ss_i \right] dr \tag{2.21}$$

When Φ is independent of i, which is a reasonable assumption for a case of a small integration period, we have

$$\langle S_{VB} \rangle = \left(\frac{K_{TR} G_{TM}}{K_M} \right)^2 \langle Ss \rangle \frac{1}{r_w} \int_r^{r+r_w} \Phi \, dr \tag{2.22}$$

where

$$\langle Ss \rangle = \frac{1}{m} \sum_{i=1}^{m} Ss_i \tag{2.23}$$

is the average bottom scattering strength.
In the case of sharp beam, we have (Aoyama *et al*. 1997)

$$\begin{aligned} \int_r^{r+r_w} \Phi \, dr &= \Phi_o \frac{c\tau}{2} \\ \Phi_o &= \int_0^{2\pi} \int_0^{\pi/2} b^2 \, \theta \, d\theta \, d\phi \end{aligned} \tag{2.24}$$

where Φ_o is the asymptotic value of the equivalent beam angle for the surface scattering. We find from Eq. (2.24) :

$$\Phi_o \cong \Psi \, . \tag{2.25}$$

Introducing Eq.(2.25) into Eq. (2.22), we get

$$\langle S_{VB} \rangle = \frac{{K_{TR}}^2 {G_{TM}}^2 \Phi_o c\tau / 2 \langle Ss \rangle}{({K_{TR}}^2 {G_{TM}}^2 \Psi \, c\tau / 2)' r_w} \tag{2.26}$$

where the prime means values which should be given to the underwater acoustic instrument as parameters. Finally we have

$$\langle Ss \rangle = r_w \langle S_{VB} \rangle \, , \tag{2.27}$$

if the parameter values have no error. This is the simple relationship between the average SS and the bottom SV.

2.5 Simultaneous display of fish and bottom scattering

Using the RSS Model we have a relationship between the raw (or not averaged) SV value of the bottom echo, S_{VB} , and the raw bottom backscattering strength, S_S, as

$$S_S = \frac{S_{VB}\,\Psi(c\,\tau\,/\,2)}{\Phi} \tag{2.28}$$

where Φ and Ψ are the equivalent beam angle for surface and volume scattering, respectively, c is the sound speed, and τ is the pulse width. At the peak of the bottom echo, we have

$$\Phi = \Phi_0 \cong \Psi \tag{2.29}$$

where Φ_o is the asymptotic value of the equivalent beam angle for surface scattering (Fig. 2.4). Introducing Eq. (2.29) into Eq. (2.28) gives

$$S_S = (c\,\tau\,/\,2)\,S_{VB} \tag{2.30}$$

and we can easily convert the raw SV to raw SS. An application of this formula for all S_{VB} yields a convenient measure called "instantaneous" SS. Figure 2.5 show the raw SV of bottom echo (S_{VB}), raw SS (S_S), and instantaneous SS.
In decibel unit,

$$SS = 10\log(c\,\tau\,/\,2) + SV_B \tag{2.31}$$

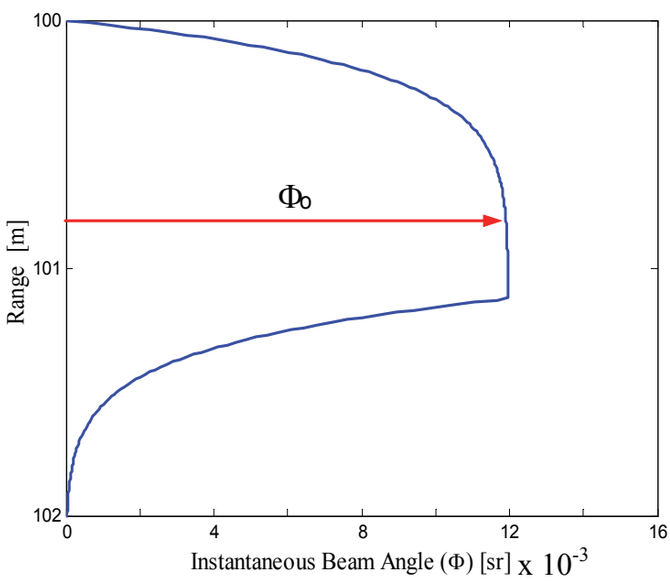

Fig. 2.4. The instantaneous equivalent beam angle $\Phi$and the asymptotic value of Φ_o.

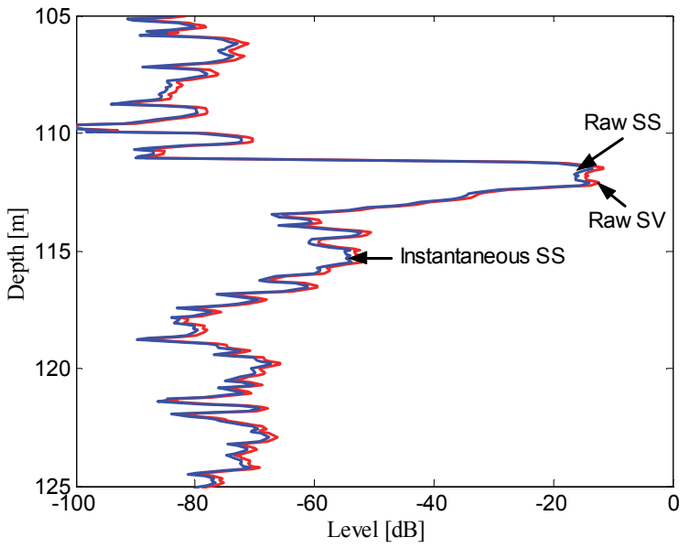

Fig. 2.5. The raw SV, raw SS, and instantaneous SS.

3. Survey methods

The echo sounder is employed in this survey to explore fish resources, bottom topography, and bottom backscattering strength. Additional instrument, such as Global Positioning System (GPS) and data storage are included as part of the acoustic system. The raw data of echo sounder is processed using Echoview and Matlab program. The sphere calibration was conducted to guarantee a high quality of acoustic data (Fig. 3.1).

Bottom material sampling using an anchor dredge was conducted to interpret the bottom echo. The obtained bottom material was saved for further processing in laboratory. The acoustic data collection and the bottom material sampling were conducted simultaneously. The bottom material was analyzed using the sieving and pipette methods. Then, the analysis of particle size was done using Wentworth scale.

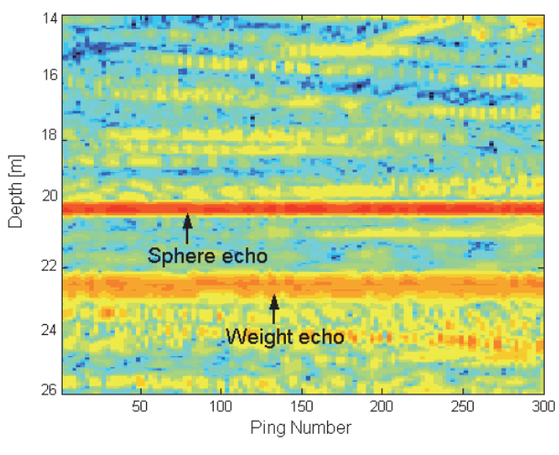

Fig. 3.1. The sphere echo during calibration.

4. Results and discussions

4.1 Bottom echo characteristics

It is shown that the underwater acoustic instrument can rather easily measures echoes by reflection of sounding pulses from the bottom. The sounder is especially useful when both fish and sea bottom should be quantified. The quantitative echogram of the It is shown that the underwater acoustic instrument can rather easily measures echoes by reflection of sounding pulses from the bottom. The sounder is especially useful when both fish and sea bottom should be quantified. The quantitative echogram of the echosounder showing raw SV as shown in Fig. 4.1 enables us to interpret the backscattered signal from any object. showing raw SV as shown in Fig. 4.1 enables us to interpret the backscattered signal from any object.

Figure 4.1 shows typical echograms at 38 kHz for sand, silt, and clay seabed. The scale shows the raw SV value ranging from -70 to -10 dB. The red belts represent the sea bottom. Because of the same range width of the echograms we can easily compare the bottom echoes and find that the thickness of the reddish belts for sand is thinner than those of silt and clay bottoms; this mainly comes from the difference of the bottom depth rather than of bottom material as discussed later.

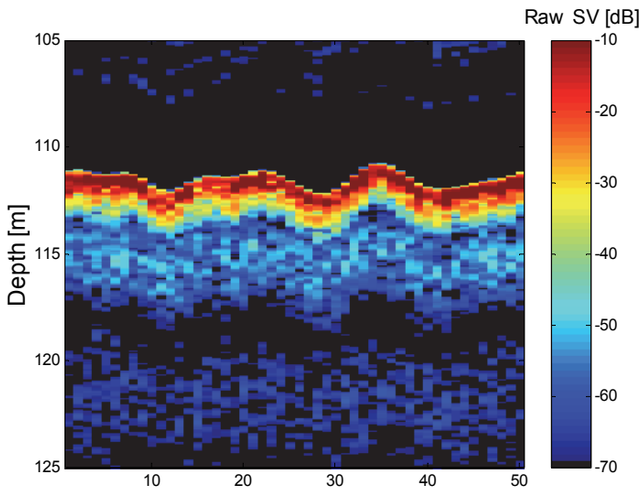

(a) Sand

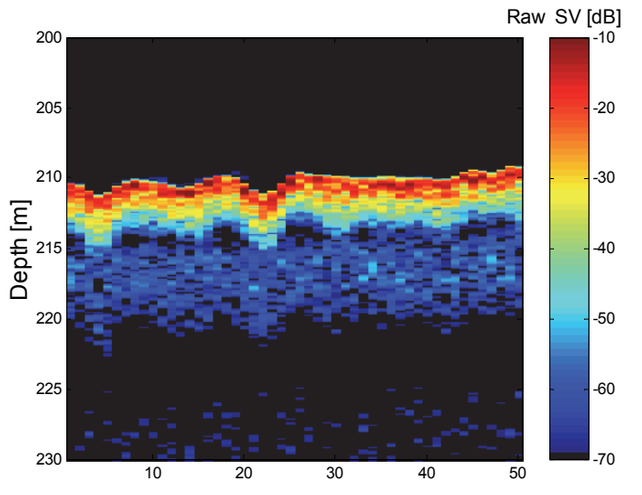

(b) Silt

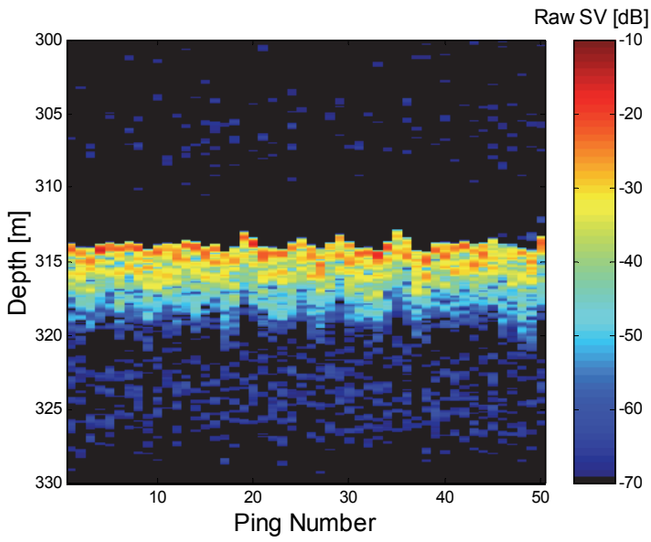

(c) Clay

Fig. 4.1. Typical echograms in raw SV for sand, silt, and clay. The range width and ping number are the same for three figures.

Figure 4.1 shows the bottom echoes in the same range scale width and easily reveals differences or similarity among the three echograms. The first red belts correspond to the contribution from the main lobe as can be seen from the simulation results in Fig. 4.2; the difference in the thicknesses comes from the depth differences but not from the material differences. We also observe two or three more weaker bluish belts beneath the main belt and these are contributions from side lobe(s) as also can be seen from Fig. 4.2.
Figure 4.2 shows several typical wave forms of the bottom echoes, with absolute raw SV scale for the three frequencies and the three materials near the points whose echograms are shown in Fig. 4.1. Figure 4.2 also shows the simulated wave forms by Eq. (2.18) using the SS values of each bottom type shown in each figure : the SS values were obtained from the peak raw SV values of bottom echo and giving Ψ, Φ, c, and τ using Eq. (2.28). At the peak of bottom echo, the echo level of sand was higher than silt and clay by more than 8 dB.
As shown in Fig. 4.2, the model calculations and measurements agree rather well in the wave form. The width change of the bottom echo was caused by the increasing depth. The bottom material is reflected only in the SS value in the present model. It was supported by the simulation results that the beam spreading caused the increase of the bottom echo width with increasing depth. The present model can well predict the scattering by the side lobes ; this figure also shows that the narrow beam and short pulse configuration receives the contributions of the bottom echoes separately by the side lobes. Comparing with the more thorough model as by Chotiros (Chotiros, 1994), this model can be used easily, sacrificing a little bit rigorousness.

4.2 Examination of bottom echo integration method

This section describes the examination of the bottom echo integration method. We examined the relation of measured bottom backscattering strength (SS) on integration width r_w for the three bottom materials of sand, silt, and clay (Fig. 4.3).

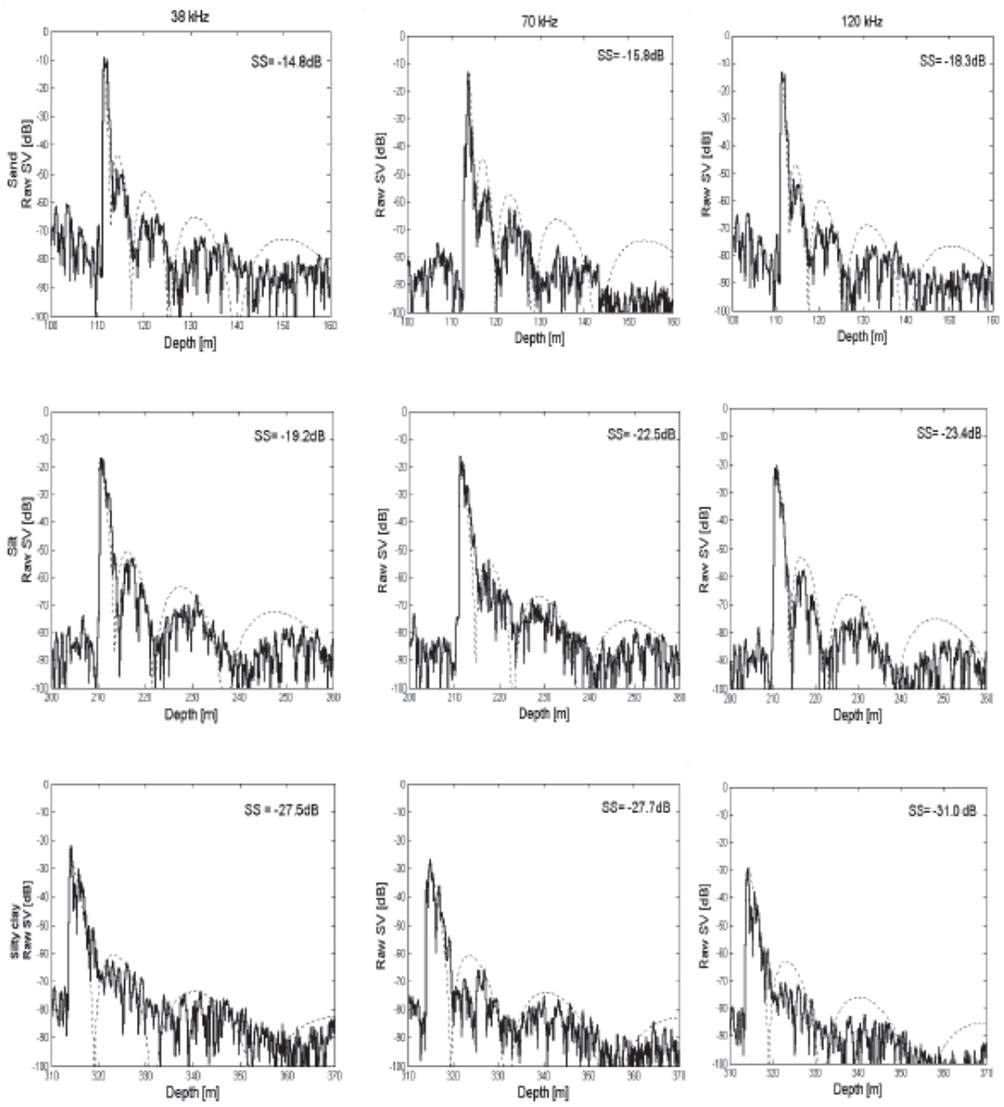

Fig. 4.2. Wave forms of sand (top), silt (middle), and clay (bottom) in raw SV by measurements (—) and simulations (-----) at 38 kHz (left), 70 kHz (middle), and 120 kHz (right).

We find from Fig. 4.3, the average SS values by the bottom echo integration are independent from the change of integration layer, r_w.

The concept of SA was originally developed for estimating the fish biomass by acoustic method. For the echo integration, the received signal is once converted to through the volume backscattering strength, S_V. The integration of S_V over the range interval [r_1, r_2] is called the area backscattering strength S_A

$$S_A = \int_{r_1}^{r_2} S_v \, dr \tag{4.1}$$

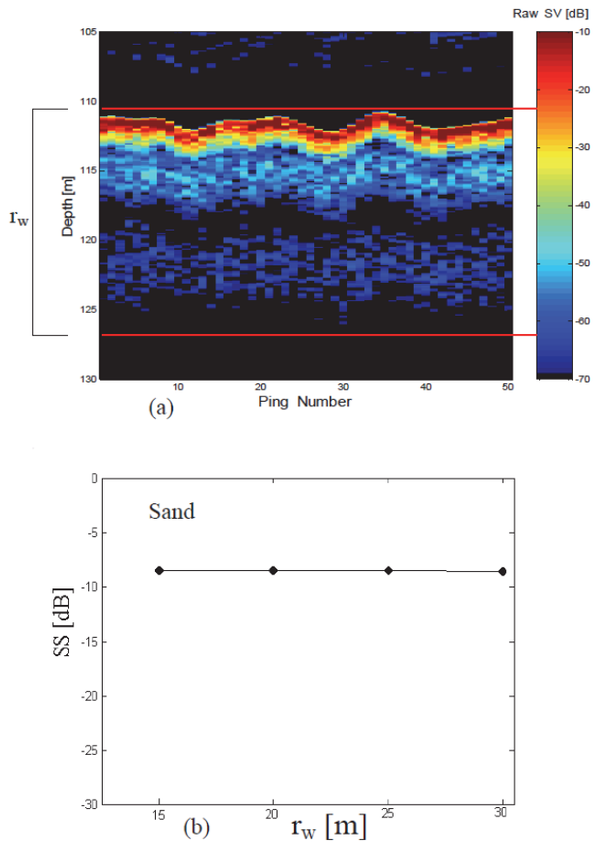

Fig. 4.3. The echogram in raw SV scale (a) and the relation of measured SS on r_w values (b).

In decibel scale $SA = 10 \log S_A$.
From Eq. (4.1) we have

$$S_A = \Sigma\, r_w \langle S_V \rangle \tag{4.2}$$

for the actual processing in which average SV, that is $\langle S_V \rangle$, are computed for each integration cell.
By Eq. (4.2) and Eq. (2.27) yields for one layer

$$S_A = r_w \langle S_V \rangle = \langle S_S \rangle \tag{4.3}$$

We find that the average SS value $\langle SS \rangle$, is equivalent to the area backscattering strength of the bottom echo (SA). Therefore, we can easily get the value by the normal function of the echo integration by selecting a belt like integration layer including the bottom echo.

4.3 Comparison of ring surface scattering model and the bottom echo integration

Comparison of the SS values by the ring surface scattering (RSS) model as shown in Fig. 4.2 and bottom echo integration methods by Eq. (2.27) are shown in Table 4.1 to confirm a good agreement. The SS values were obtained from the peak raw SV values of bottom echo and giving Ψ, Φ, c, and τ using Eq. (2.28). The average SS by the bottom echo integration (BEI) model used the integration period of 0.1 nmi.

4.4 Frequency characteristics of bottom scattering backstrength

We examine the frequency characteristics of the bottom scattering backstrength by underwater acoustic instrument frequencies of 38, 70, and 120 kHz. The multi-frequency approach will increase the accuracy of the target (sea bottom) estimation due to different response of the target to the frequencies used.

Figure 4.4 shows the average SS for 100 number of data and standard deviation of the SS as a function of frequencies for each bottom type. The standard deviation is obtained by taking the root mean square (RMS) deviation of the average SS. There are several same data of mean diameter particle. The SS decreases with increasing frequency (Fig. 4.4). The results show that the SS for 38 kHz are 2 to 3 dB greater than for 70 and 120 kHz. This is consistent with the conclusions of Stanic *et al.,* (1988) who showed that the SS at normal incidence decreased with increasing frequency by 1.5 dB.

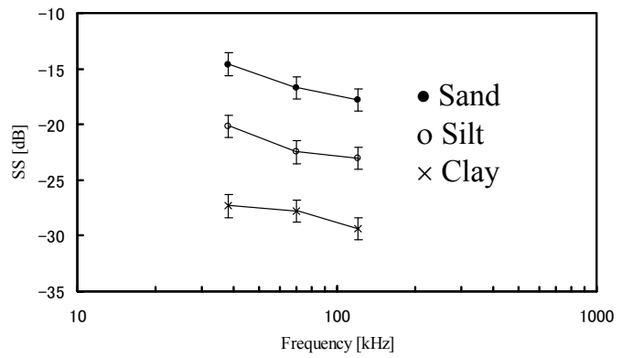

Fig. 4.4. Frequency dependence of measured bottom backscattering strength for sand, silt, and clay with ± 1 standard deviation indicated.

Bottom material	SS [dB]								
	38 kHz			70 kHz			120 kHz		
	BEI	RSS	Δ	BEI	RSS	Δ	BEI	RSS	Δ
Sand	-12.6	-12.8	0.2	-15.7	-15.8	0.1	-18.8	-19.3	0.5
Silt	-21.2	-20.2	1.0	-22.6	- 22.6	0	-24.0	-24.4	0.4
Clay	-28.3	-28.5	0.2	-28.8	- 28.7	0.1	-29.4	- 31.4	1.0

Table 4.1. The average SS values obtained by bottom echo integration method (BEI) and ring surface scattering (RSS) method and the difference (Δ=BEI-RSS). The number of data for each bottom type is 100.

4.5 Bottom material characteristics

Ten bottom material samplings were conducted during the survey. The bottom materials of sand, silt, and clay were determined observing physical characteristics of the samples and mean diameter values. Particle size analysis were conducted by Wentworth scale. The mean

diameter of the bottom materials from each 100 data are 223 to 301 μm for sand, 58 μm for silt, 36 to 43 μm for sand-silt-clay, and 9 to 10 μm for clay.
To examine the correlation with bottom properties, the measured average (integrated) SS values were plotted against the mean diameter of the bottom material (Fig. 4.5). The regression line shown is given by

$$SS\ [\mathrm{dB}] = 9.0 \log_{10} (d\ [\mu\mathrm{m}]) - 45.8 \tag{4.4}$$

with a high correlation coefficient of 0.98, where d is mean diameter of particle size in μm. The data were merged for frequencies in the regression because of the small frequency dependence, but the frequencies are discriminated in Fig. 4.5. The larger the grain size, the stronger the bottom backscattering strength.

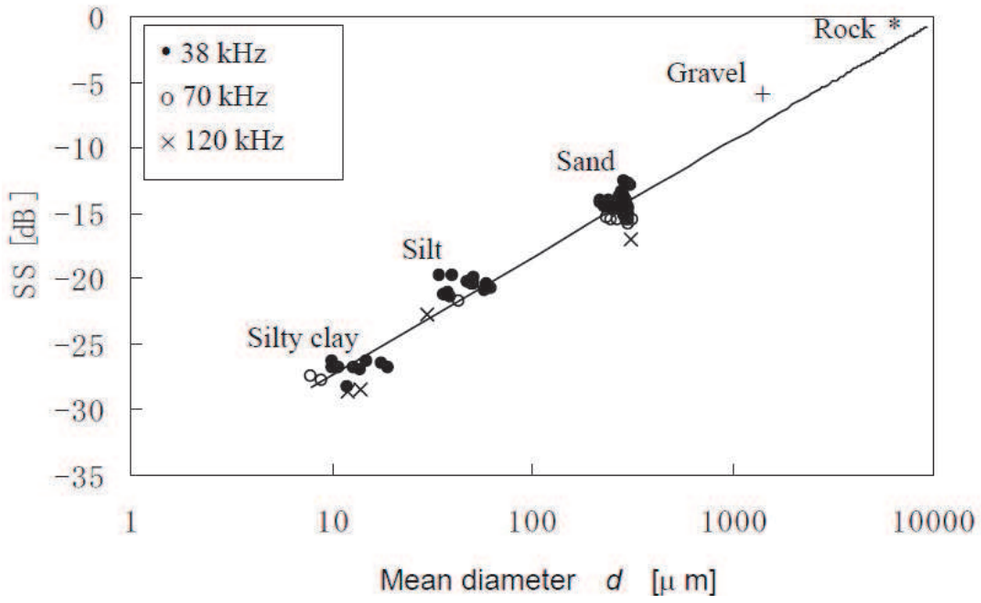

Fig. 4.5. Bottom particle diameter dependence of bottom backscattering strength. The regression line and correlation coefficient, r_c, are indicated.

An increase in mean diameter is accompanied by a higher backscattering strength (Fig.4.5). The reason for this is related to the bulk density of the sediments. The sand (grain sizes from 62 to 2000 μm, from the smooth sand to coarsest sand) has a bulk density between 1.9 and 2.1 g/cm^3, silt and clay (grain sizes < 62 μm) have much lower values of bulk density, usually varying between 1.2 and 1.6 g/cm^3. The bulk density of the sediment is determined principally from porosity. The porosity values of silt and clay are higher than sand; this is due to the fact that the silt and clay bind water more than the sand. Therefore, there are more water-filled voids per given volume of silt and clay than sand. Bulk density determines the acoustic impedance of sediment ; the higher the sediment density, the higher the impedance, and the greater the scattering backstrength.
As shown in Figs. 4.4, and 4.5 the average SS of sand is higher than silt and clay by more than 5 dB. To some extent, it was possible to relate SS to mean diameter, suggesting the possibility of bottom type classification. We examined our regression to estimate the bottom backscattering strength (SS) for rock and gravel. For this purpose, the regression line is

extended without disturbing the original data. By our regression, the estimated SS is -1.3 dB for rock with diameter 8 mm. Urick (Urick,1954) used frequency of 55 kHz and found the SS of rock is -0.8 dB. The estimated SS is -6.7 dB for gravel with diameter 2 mm. The measured SS for gravel is -7.8 dB (Applied Physics Laboratory, UW, 1994).
Although the present data lack particle sizes from 70 μ m to 220 μ m, further investigation is necessary to clarify the particle size dependence of SS, Fig. 4.5 or Eq. (4.4) gives a guide to relate the SS and the bottom material.

5. Bottom survey off java island

5.1 Sea bottom depth measurement

The echo sounder measured sea bottom depths and the result of the quantitative echogram in instantaneous SS scale is shown in Fig. 5.1 as examples.
The maps show that most of the floors have irregular topography and that the surveyed areas were steeply sloping bottom. According to the depth, the survey area is the continental shelf and the other survey areas are the continental slopes. These are due to that the bottom morphology of this areas are mostly consists of troughs.

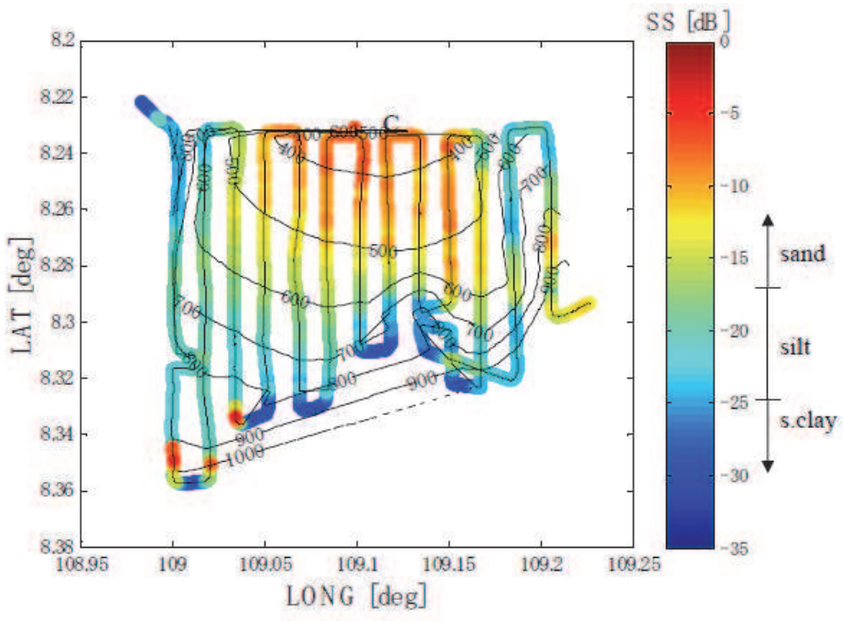

Fig. 5.1. The acoustic track, the bathymetry map (a) and SS distribution (b).

5.2 Bottom backscattering strength by bottom echo integration

The measurement of bottom backscattering strength (SS) using the bottom echo integration method along the acoustic track were conducted. The bottom echo integration (BEI) method measures the average bottom SS by averaging the bottom echoes for a predefined depth layer including the bottom echoes and ping sequence. We found that this process is theoretically same to the ordinary process of the echo integration to get the area backscattering strength (SA) and that the average bottom SS can be easily obtained by a commercial software such as Echoview. The SS map results for the integration period of 0.1

nmi of bottom echo are shown in Fig. 5.1. together with depth contour. The general correlation between SS and depth contour for the present survey was the increasing depth followed by decreasing SS. Figure 5.2 show the bottom trawling, SS distribution, and detected fish school (●) of the survey area.

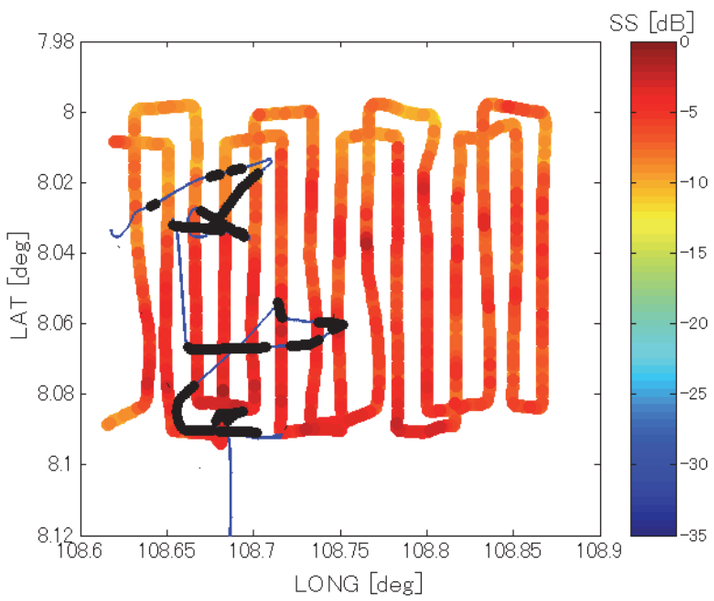

Fig. 5.2. The bottom trawling (—), SS distribution, and detected fish school (●) of survey area

5.3 Identifying bottom material by the SS value and relate it to fish habitat

This section shows an investigation of the relationship between sea bottom material and fish close to sea bottom information obtained by using echo sounder. From the bottom surface to upper depth is SV value and to the lower depth is instantaneous SS.

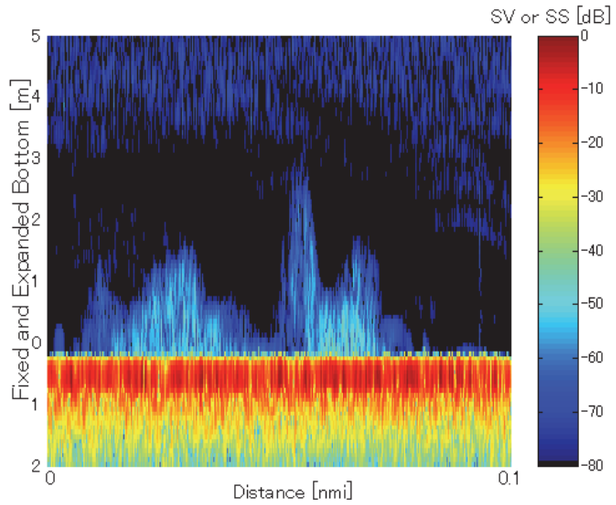

Fig. 5.3. Measured scattering strength of fish (SV) close to the sea bottom and the SS sea bottom.

Figure 5.3 shows simultaneously the scattering from fish school (SV) close to the sea bottom and the SS values by RSS model (Eq. (2.30)) as the fixed and expanded bottom at trawl survey area. The example of echograms is shown in Fig. 5.3. The increasing of fish density is followed by the increasing receiving voltage of acoustic instrument (Fig. 5.4).
The estimated bottom material is conducted by the SS value.In our results,, the SS value higher than -14.0 dB we categorized as a sand. The SS lied between – 20.0 to -15.0 dB is the silt and the SS less than -22.0 dB is as clay.

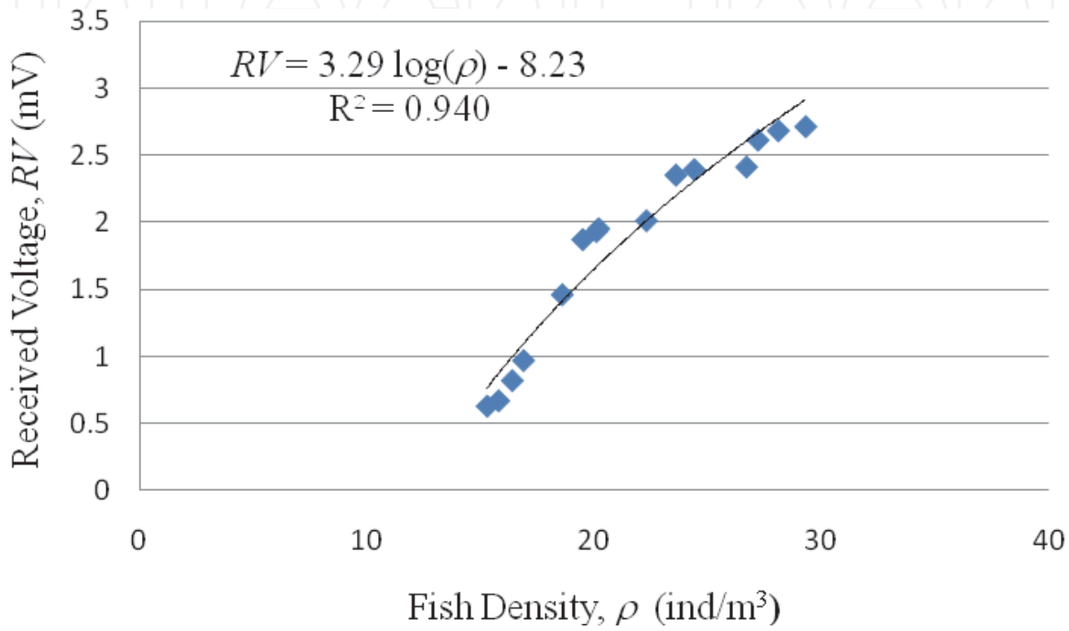

Fig. 5.4. The relationship between received acoustic voltage and fish density.

5.4 Consideration

The bottom material is estimated by the SS value. The measured SS is about -12.0 to -5.0 dB when the bottom fish schools were existences. By this value, the bottom material is estimated as sand. The measured SS is about -28.0 to -16.0 dB when the bottom fish schools were absent. The bottom material is estimated as silt and clay, respectively. From this results, the bottom fish schools tend to be associated with the main areas of sand. This interpretation is also supported by the trawl data showing the fish caught in this sand area. The scattering from fish (SV) and bottom (SS) are simultaneously display in echogram. Among the total 98 fish schools examined 95 schools were on the sand bottom. The SV values of fish close to the sea bottom are ranging from -70.0 to -35.0 dB.
The distribution of fish reflect variability in the surrounding environment, and those area normally occupied by a species constitute its habitat. Generally, individual species are not ubiquitous, suggesting that habitat is restrictive.
Bottom type has a major influence on the fish distribution patterns (Gibson and Robb, 1992;). Bottom type preference related to the distribution of suitable prey and the ability of fish to effectively bury themselves, which means they are protected from predation and achieve a strategic advantage in feeding (Gibson and Robb, 1992).

There may also be important differences in the availability and quality of bottom fish associated with different bottom (Gray, 1974). He reported that fish are abundant in sand and decreases in abundance in the silt and clay. The highest densities of fish in sand, since sand are stable from water currents. The other fish is abundant in silt and clay in which they feed. Our case fish is abundant in sand, may be for their living and burying to protect from predation, but further investigation is necessary.

6. Conclusions

The quantification technique of echoes using underwater acoustic instrument can rather easily measure echoes by reflection of sounding pulses from fish and sea bottom.
The conclusions from the results of the experiments, assessment, and analysis performed in this study are described below :

1. Underwater acoustic instrument is a reliable tool to measure bottom backscattering strength and useful when to observe both fish and sea bottom ;
2. The ring surface scattering (RSS) model expressed by the instantaneous equivalent beam angle can well predict echo shapes of the actual bottom echo ;
3. Higher bottom backscattering strength is followed by the higher mean diameter of particle as shown by Eq. (4.4) ;
4. The bottom backscattering strength a little bit decreases with increasing frequency ;
5. The SS is independent with the integration width, r_w ;
6. The area backscattering strength (SA) is equivalent to the bottom backscattering strength (SS);
7. The RSS model is able to measure the SS and the result is nearly equal with the bottom echo integration model ;
8. The bottom material sampling in the study area show that bottom type is sand, silt, sand-silt-clay, and clay.
9. The bottom fish were existence with the sand bottom material ;
10. The bottom echo integration (BEI) model enables us to study bottom material in the synoptic area while the RSS model for bottom material in detail beneath the specified fish.

7. Acknowledgment

The research was supported by Directorate General of Higher Education Ministry of National Education Indonesia and Japan Society for the Promotion of Science (JSPS).

8. References

Aoyama, C., E. Hamada, M. Furusawa, K. Saito. (1997). Calibration of Quantitative Echo Sounders by Using Echoes from Water Tank Surface, *Nippon Suisan Gakkaishi*.; 63:570-577. (*in Japanese*).

Aoyama, C, E. Hamada, M. Furusawa. (1999). Total Performance Check of Quantitative Echo Sounders by Using Echoes from Sea Bottom. *Nippon Suisan Gakkaishi*, 65(1), 78-85 (*in Japanese*).

Applied Physics Laboratory, University of Washington. (1994). High Frequency Ocean Environmental Acoustic Models Handbook.

Chotiros, N.P. (1994). Reflection and reverberation in normal incidence echo sounding. *J. Acoust. Soc. Am.*; 96: 2921-2929.

Eckart, C. (1953). The scattering of sound from the sea surface. : *J. Acoust. Soc. Am.*; 25: 566-570.

Furusawa, M. (2000). New technologies for quantitative echo sounders. Meeting of Scientific Committee for Ocean Research (SCOR).

Gibson, R.N., Robb, L. (1992). The relationship between body size, sediment grain size and burying ability of juvenile plaice. Fish Biol. 40, 771-778.

Gray, J.S. (1974). Animal-sediment relationships. Oceanogr. Mar. Biol. Annu. Rev. 12:222-261.

Jackson, D.R, S.P. Winebrenner, and A. Ishimaru. (1986). Application of composite roughness model to high frequency bottom scattering. *J. Acoust. Soc. Am.*; 79: 1410-1422.

MacKenzie, K.V. (1961). Long range shallow water bottom reverberation. *J. Acoust. Soc. Am.* 34. 62.

MacLennan, D.N and E.J. Simmonds. (1992). *Fisheries Acoustics*, Chapman & Hall, ISBN-13: 978-0-632-05994-2. London.

McKinney, C.M and C.D. Anderson. (1964). Measurements of backscattering of sound from ocean bottom. *J. Acoust. Soc. Am*. 36. 1.

Stanic, S., Briggs, K.B., Fleischer, P., Sawyer, W.B. and Ray, R.I. (1989). High Frequency Acoustic Backscattering from a Coarse Shell Ocean Bottom. *J. Acoust. Soc. Am*. 85: 125-136.

Stanton,T.K : Sound scattering by marine objects. (1994). Lecture Notes. Meeting of Marine Acoustic Society of Japan. 21(4).

Stanton, T.K. : Sea surface scattering - Echo PDF. (1985). *J. Acoust. Soc. Am*. 77: 1367-1369.

Urick, R.J. (1954). The backscattering of sound from a harbor bottom. *J. Acoust. Soc. Am*. 26. 231.

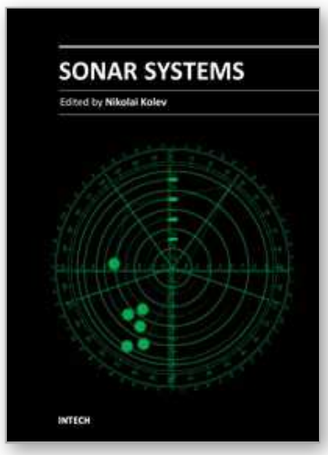

Sonar Systems

Edited by Prof. Nikolai Kolev

ISBN 978-953-307-345-3
Hard cover, 322 pages
Publisher InTech
Published online 12, September, 2011
Published in print edition September, 2011

The book is an edited collection of research articles covering the current state of sonar systems, the signal processing methods and their applications prepared by experts in the field. The first section is dedicated to the theory and applications of innovative synthetic aperture, interferometric, multistatic sonars and modeling and simulation. Special section in the book is dedicated to sonar signal processing methods covering: passive sonar array beamforming, direction of arrival estimation, signal detection and classification using DEMON and LOFAR principles, adaptive matched field signal processing. The image processing techniques include: image denoising, detection and classification of artificial mine like objects and application of hidden Markov model and artificial neural networks for signal classification. The biology applications include the analysis of biosonar capabilities and underwater sound influence on human hearing. The marine science applications include fish species target strength modeling, identification and discrimination from bottom scattering and pelagic biomass neural network estimation methods. Marine geology has place in the book with geomorphological parameters estimation from side scan sonar images. The book will be interesting not only for specialists in the area but also for readers as a guide in sonar systems principles of operation, signal processing methods and marine applications.

InTech Europe
University Campus STeP Ri
Slavka Krautzeka 83/A
51000 Rijeka, Croatia
Phone: +385 (51) 770 447
Fax: +385 (51) 686 166
www.intechopen.com

InTech China
Unit 405, Office Block, Hotel Equatorial Shanghai
No.65, Yan An Road (West), Shanghai, 200040, China
中国上海市延安西路65号上海国际贵都大饭店办公楼405单元
Phone: +86-21-62489820
Fax: +86-21-62489821

IntechOpen